Ligand isotope structure of the optical $^7F_0 \rightarrow {}^5D_0$ transition in $EuCl_3 \cdot 6H_2O$

R. L. Ahlefeldt, A. Smith, and M. J. Sellars
Laser Physics Centre, Research School of Physics and Engineering, The Australian National University, Canberra, Australian Capital Territory 0200, Australia

(Received 23 August 2009; published 5 November 2009)

The structure of the $^7F_0 \rightarrow {}^5D_0$ transition of Eu^{3+} in $EuCl_3 \cdot 6H_2O$ is investigated in crystals with three different isotopic compositions [natural abundance (0.2% ^{18}O, 0.01% ^2H), 1.9% ^{18}O, and 0.06% ^2H]. Raman-heterodyne-detected NMR is used to identify shifts caused by isotopes of the ligands O and H in sites neighboring the Eu site in the lattice. The structure of the $^7F_0 \rightarrow {}^5D_0$ transition is explained as a combination of the hyperfine structure of ^{151}Eu and ^{153}Eu and isotope shifts caused by Cl, O, and H.

DOI: 10.1103/PhysRevB.80.205106 PACS number(s): 78.40.Ha, 76.70.Hb, 61.72.−y

I. INTRODUCTION

Rare-earth optical centers in crystals have properties highly desirable for ensemble-based quantum information devices such as optical quantum memories and quantum repeaters. These properties include observed coherence times as long as 14 ms for optical transitions[1] and 30 s for hyperfine transitions.[2] However, creating ensembles with the narrow inhomogeneous linewidths and high optical densities required is difficult. A number of quantum memory demonstration experiments have been carried out using optical pumping techniques to select a narrow ensemble from a broad inhomogeneous line.[3–6] The crystals used in these experiments had inhomogeneous linewidths on the order of gigahertz, whereas the selected ensembles had sub-megahertz linewidths. Although useful for demonstrations, optical pumping techniques severely constrain the bandwidth and efficiency of the quantum memory. A more satisfactory solution is to find materials with intrinsically small inhomogeneous linewidths.

Inhomogeneous broadening on optical transitions in solids is caused by disorder in the lattice. The disorder can have many sources, including intrinsic defects, impurities, and macroscopic strain in the crystal. The optical center itself is a source of disorder in doped crystals. Strong interactions between neighboring dopant ions shift transition frequencies, resulting in satellite lines in the spectrum. Smaller shifts occur for more distant dopants and the overlap of many of these small shifts results in concentration-dependent inhomogeneous broadening. Obtaining low inhomogeneous broadening in doped crystals often requires very low dopant concentrations and hence low optical densities. If a crystal has a very low dopant concentration and other sources of disorder are absent, the existence of isotope shifts caused by ligand isotopes in the crystal can become the major residual broadening mechanism. Agladze *et al.*[7] showed that ^6Li and ^7Li in the immediate environment of Ho^{3+} in $YLiF_3$ lead to satellite structure on optical transitions. Linewidths as low as 10 MHz have been achieved in isotopically pure Y $^7LiF_4$ containing ppm concentrations of Nd^{3+} (Ref. 8) and Er^{3+} (Ref. 9).

In this paper we present an investigation into the contribution of isotopes to the structure and inhomogeneous broadening in europium chloride hexahydrate ($EuCl_3 \cdot 6H_2O$), a stoichiometric crystal with very low inhomogeneous broadening. Stoichiometric crystals are of interest for quantum memories because they have high optical densities and optical centers that do not introduce disorder into the lattice, unlike doped crystals. In a stoichiometric crystal, therefore, it is possible to achieve a high optical density and low inhomogeneous broadening concurrently.

The $^7F_0 \rightarrow {}^5D_0$ transition of Eu^{3+} in $EuCl_3 \cdot 6H_2O$ has a total linewidth of $\approx$600 MHz and exhibits a partially resolved structure, with a width for each component of $\approx$100 MHz. This narrow optical linewidth in a material that is not isotopically pure raises the possibility that the linewidth could be substantially reduced by using isotopically pure starting materials.

In $EuCl_3 \cdot 6H_2O$ the single Eu^{3+} ion site has C_2 symmetry and is surrounded by six H_2O molecules and two Cl^- ions in a slightly distorted square antiprism arrangement.[10] Each of the ligand elements has multiple naturally occurring stable isotopes: there are two isotopes of chlorine [^{35}Cl(76%) and ^{37}Cl(24%)] three of oxygen [^{16}O(99.76%), ^{17}O(0.04%), and ^{18}O(0.2%)] and two of hydrogen [^1H(99.99%) and ^2H(0.01%)]. Europium has two isotopes, ^{151}Eu(48%) and ^{153}Eu(52%), both with nuclear spin $I=\frac{5}{2}$. The singlet states $^7F_0$ and $^5D_0$ are split into three hyperfine levels with the splitting determined by the electric quadrupole and pseudoquadrupole interactions. The hyperfine structure of both isotopes is on the order of 100 MHz.

The hyperfine structure of both Eu isotopes and the expected ligand isotope shifts in the $^7F_0 \rightarrow {}^5D_0$ transition in $EuCl_3 \cdot 6H_2O$ are of the same order as the inhomogeneous linewidth, resulting in a complex structure with many partially resolved components. In order to separate these components Raman heterodyne detection of NMR was used. Raman heterodyne detection of NMR can be used in a three-level system when all three transitions between the levels are allowed.[11] A laser field is used to induce coherence between two levels separated by an optical transition and an rf field induces coherence between two levels separated by a hyperfine transition (either ground or excited state). Coherent emission occurs at the sum or difference in the rf and laser frequencies and is detected as a beat on the transmitted laser field. Raman heterodyne detection of NMR has a much faster time response than more conventional optical detection of NMR, where incoherent emission is detected, making high rf

resolution possible at fast rf scan speeds. This made it possible to rapidly construct two-dimensional (2D) maps of the NMR signal as a function of both rf and optical frequency. Yamaguchi and Suemoto have demonstrated that two-dimensional maps constructed using double-resonance techniques (in their case ODNMR, instead of Raman heterodyne NMR) are useful for identifying satellite peaks in crystals where many peaks overlap in the excitation spectrum, such as $Eu^{3+}:Y_2O_3$ (Ref. 12).

II. METHOD

Single crystals of $EuCl_3 \cdot 6H_2O$ were grown from a water solution using 99.999% pure $EuCl_3 \cdot 6H_2O$ starting material (American Elements). A natural abundance (0.2% ^{18}O, 0.01% ^{2}H) crystal was grown, and $H_2{}^{18}O$ and $^{2}H_2O$ were used to grow a 1.9% ^{18}O-doped sample and a 0.06% ^{2}H-doped sample, respectively. The crystals were typically $\approx 10 \times 8 \times 3$ mm.

Excitation and Raman heterodyne double-resonance spectra were recorded using a Coherent 699–29 ring dye laser with a linewidth of 1 MHz. As $EuCl_3 \cdot 6H_2O$ is highly hygroscopic and unstable in vacuum, the samples were placed in a small helium-filled chamber within a liquid-helium bath cryostat. For excitation spectra the $^7F_0 \rightarrow {}^5D_0$ transition at 579.7 nm was excited and emission to the ^7F levels at >600 nm was collected using a photomultiplier tube with a low-pass filter. These crystals have extremely high optical densities. To avoid significant distortion of the excitation spectrum due to absorption, the propagation direction of the beam was aligned close to the C_2 axis, where absorption is lowest. In addition, a confocal imaging system was used to ensure that emission was collected only from the front face of the crystal.

To record Raman heterodyne spectra the sample was mounted in a small six-turn coil. An rf signal was supplied by a HP Spectrum Analyzer connected to a 200 W power amplifier producing a 10 μT field in the sample. The transmitted beam was focused onto a 125 MHz bandwidth Si photodetector and the beat frequency was extracted by the spectrum analyzer.

III. RESULTS

An excitation spectrum of the $^7F_0 \rightarrow {}^5D_0$ transition in natural abundance $EuCl_3 \cdot 6H_2O$ is shown in Fig. 1(a). Five partially resolved peaks are visible (one as a shoulder at 250 MHz) spanning 600 MHz. These peaks are marked as region A in Fig. 1(a). A set of small amplitude, poorly resolved peaks occur at frequencies between −500 and −1300 MHz (region B).

The structure of the $^7F_0 \rightarrow {}^5D_0$ transition of $EuCl_3 \cdot 6H_2O$ was previously studied by Martin *et al.*,[13] who attributed it to a combination of the hyperfine structure of ^{151}Eu and ^{153}Eu. However, the small peaks in region B were not visible in the spectrum presented by Martin *et al.* due to the high inhomogeneous broadening in their sample. These small peaks cannot be explained by the hyperfine structure, and we, therefore, considered it worthwhile to reinvestigate the structure of the entire line.

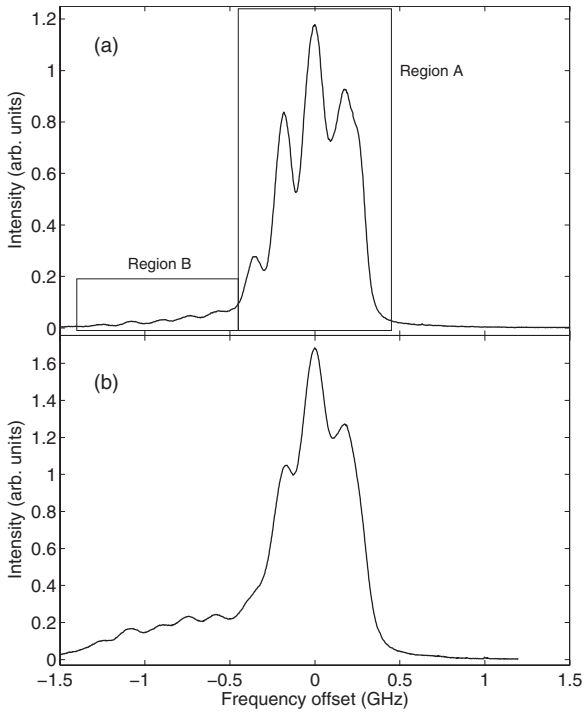

FIG. 1. $^7F_0 \rightarrow {}^5D_0$ transition in (a) $EuCl_3 \cdot 6H_2O$ with natural isotopic abundances (b) 1.9% $^{18}O:EuCl_3 \cdot 6H_2O$. In (a), region A contains the peaks of the main optical line, and region B contains the shifted peaks we show are caused by ^{18}O.

The amplitudes of the peaks in region B are consistent with an impurity ion present at a level of 0.2%–0.5%. As the only species present at this level is ^{18}O (0.2% abundance), a 1.9% ^{18}O-doped sample was grown to compare with the natural abundance sample. An excitation spectrum of this 1.9% $^{18}O:EuCl_3 \cdot 6H_2O$ sample is shown in Fig. 1(b). This spectrum shows that the region B peaks are caused by ^{18}O; the amplitudes of the peaks are higher than those of the natural abundance sample and are consistent with the concentration of ^{18}O. The higher concentration of ^{18}O also results in an additional 30 MHz of inhomogeneous broadening.

We attribute the small peaks in region B of the spectrum to the small subset of europium ions in the crystal that have an ^{18}O ion as one of their direct ligands. There are three crystallographically distinct oxygen ligand sites and the C_2 symmetry means that two identical sites contribute to each distinct site. The presence of an ^{18}O ion in one of these three sites causes a shift in the optical transition frequency of the europium ion. The three ^{18}O ion sites must cause different optical shifts because the span of the ^{18}O peaks in region B is larger than the width of the ^{16}O line (region A).

Two-dimensional Raman heterodyne double-resonance spectroscopy of the natural abundance $EuCl_3 \cdot 6H_2O$ sample was used to separate the three oxygen sites contributing to the ^{18}O peaks in region B, and to identify the contributions of other isotopes to the spectrum. Raman heterodyne double-resonance spectra about the two ground-state transitions of ^{151}Eu (26.99 and 29.03 MHz) and ^{153}Eu (74.58 and 70.07 MHz) are shown in Fig. 2. In these figures dark colors indi-

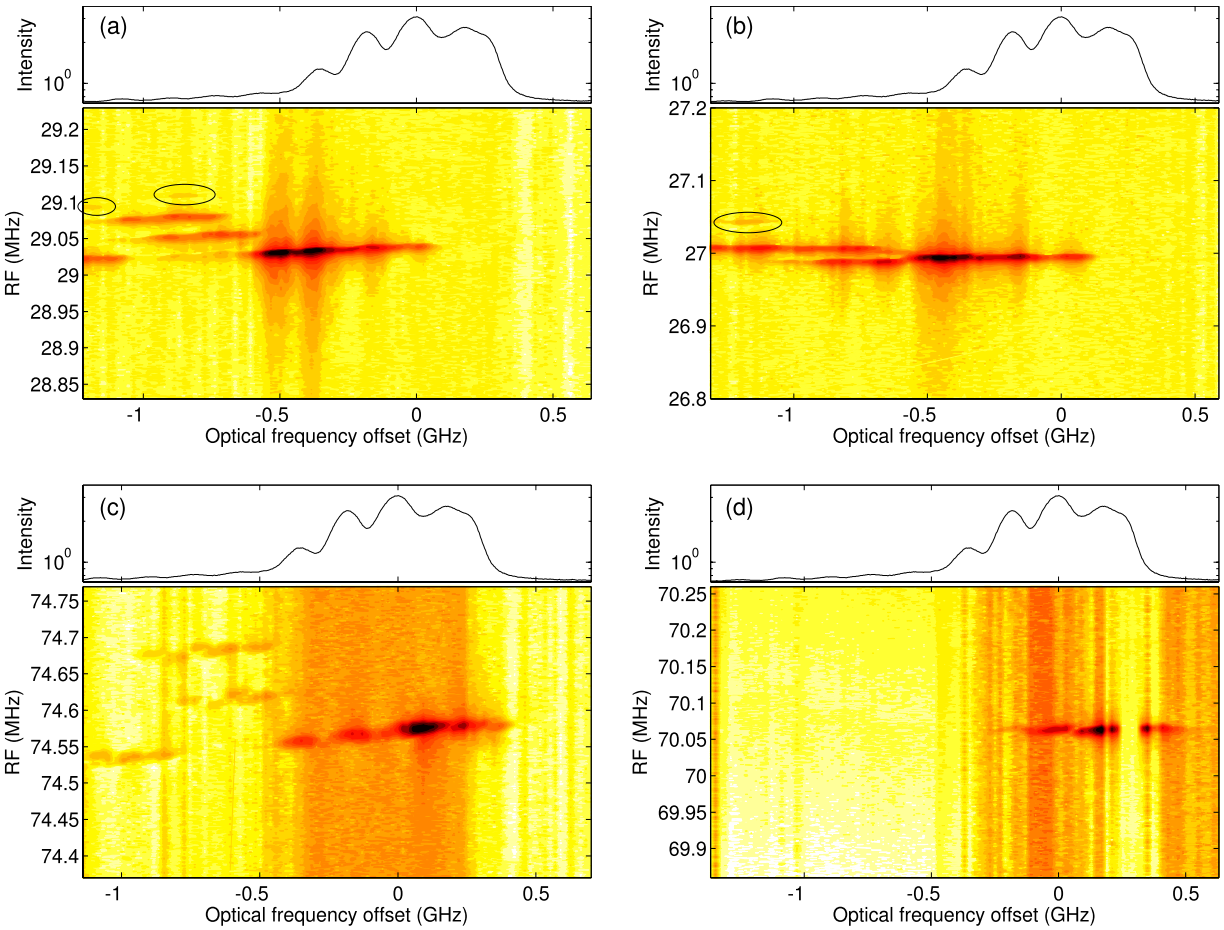

FIG. 2. (Color online) Raman heterodyne double-resonance spectra of ground-state hyperfine transitions of ^{151}Eu and ^{153}Eu. (a) 29.03 MHz transition of ^{151}Eu, (b) 26.99 MHz transition of ^{151}Eu, (c) 74.58 MHz transition of ^{153}Eu, and (d) 70.07 MHz transition of ^{153}Eu. For each transition, the excitation spectrum from Fig. 1 with a logarithmic vertical scale is displayed in the upper plot as a guide, and the Raman heterodyne double-resonance spectrum with a logarithmic color axis is shown in the lower plot. The signals from the ^{18}O peaks are weaker in the 74.58 MHz spectrum and absent in the 70.07 MHz spectrum because of larger noise at these frequencies. The circled peaks in (a) and (b) are those we have attributed to ^{2}H.

cate strong signals. The intensity of the signal in these spectra is not directly related to the density of ions with a particular transition frequency. The population dynamics, strengths of the transitions involved, and other factors strongly influence the observed intensity. The background is also dependent on a variety of factors. When the crystal hole-burns effectively and the spectral density of ions is high, such as in the center of the optical line, modulation of the hole by the rf field results in wide wings in the rf, which are pronounced in Fig. 2(c).

The main optical line gives strong Raman heterodyne signals in Figs. 2(a)–2(d). A comparison of Figs. 2(a) and 2(c) shows that there is an optical isotope shift of −200 MHz in the Raman heterodyne signal of ^{151}Eu relative to ^{153}Eu. The three ^{18}O peaks, which were overlapped in the excitation spectrum [Fig. 1(a)], are resolved in the Raman heterodyne double-resonance spectra because they have different hyperfine frequencies. The three peaks can be clearly seen in Figs. 1(a)–1(c) at optical shifts of −580, −720, and −1080 MHz relative to the high-frequency edge of the main line. They are not visible in Fig. 1(d) because there is a large amount of noise at this frequency. About the 74.58 and 29.03 MHz transitions, there are gradients in the signal across the entire spectrum of 38 ± 4 and 14 ± 3 kHz/GHz, respectively.

The main part of the optical line is due to the subset of europium ions with only ^{16}O as direct ligands. The ^{16}O signal is at least 600 MHz wide along the optical axis in all Raman heterodyne double-resonance spectra. This is much greater than the total expected width of the hyperfine splitting (130 MHz for ^{151}Eu and 320 MHz for ^{153}Eu). We propose that the wide signal is a combination of three subsets of europium ions with different combinations of chlorine isotopes as ligands. Two of the europium ligands are chlorine ions in identical sites, and three shifted subsets will arise when zero, one, or two of these sites are occupied by ^{37}Cl instead of ^{35}Cl. An optical shift of between 150 and 250 MHz caused by each ^{37}Cl ion is necessary to explain the observed width. A smaller optical frequency shift is expected for ^{37}Cl compared to ^{18}O because the chlorine isotope relative mass difference is half the oxygen isotope relative mass difference.

The circled faint peaks in Figs. 2(a) and 2(b) are 5% of the size of the ^{18}O peaks and are mostly at larger optical shifts. This suggests they are caused by ^{2}H, which has a

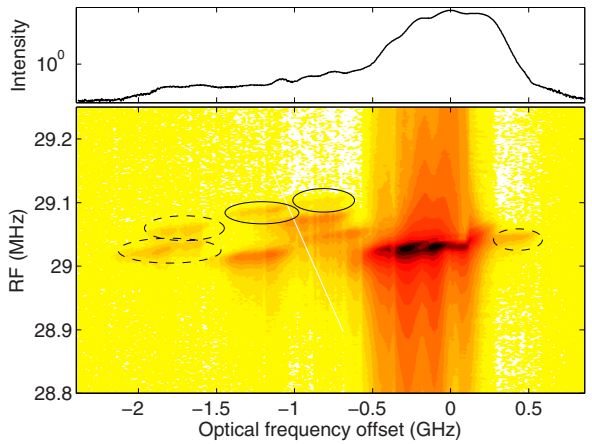

FIG. 3. (Color online) Raman heterodyne double-resonance spectrum of the 29.03 MHz ground-state transition of ^{151}Eu in 0.06% ^{2}H:$EuCl_3 \cdot 6H_2O$. The upper plot is an excitation spectrum. The solid circles indicate peaks visible in the 29 MHz spectrum of the natural abundance sample, Fig. 2(a), while the dashed circles indicate peaks not seen in that spectrum.

natural abundance of 0.01%. To confirm this, Raman heterodyne double-resonance and excitation spectra were recorded for a sample enriched to 0.06% ^{2}H and are shown in Fig. 3. Five peaks caused by ^{2}H are visible in the Raman heterodyne double-resonance spectrum. Six peaks are expected, although it is likely that the remaining peak is overlapped with an existing signal.

Because the chlorine peaks are not well separated along the rf axis in Fig. 2 it is difficult to determine the ^{37}Cl isotope shift from the Raman heterodyne double-resonance spectra. Instead, the chlorine isotope shifts were determined from a fit to the excitation spectrum, shown in Fig. 4(a). The fit is a combination of the hyperfine structure of ^{151}Eu and ^{153}Eu, including the chlorine and oxygen isotope shifts. Only the three strongest hyperfine transitions, with $\Delta m_I = 0$, are included in the fit and we assumed the same ordering of the hyperfine levels in the ground and excited states (see Fig. 5). The fit has four free parameters: the europium isotope shift, the ^{37}Cl isotope shift, the inhomogeneous broadening for each component, and an absorption parameter. The absorption parameter accounts for absorption of the incident light before it reaches the region of the crystal from which the emission is collected. The isotopic abundances of Eu, Cl, and O gave the relative heights of each component.

The fit to the observed spectrum in Fig. 4(a) is excellent, given the limited number of free parameters. There are two unexplained features: the slight wings on either side of the line are not accounted for in the model, and the oxygen peaks are 50% bigger than the model predicts. The fit gives an inhomogeneous broadening on each component of 103 MHz, a europium isotope shift of −200 MHz on ^{151}Eu relative to ^{153}Eu, and a ^{37}Cl shift of −179 MHz. A reasonable fit can still be obtained if the $\Delta m_I = 1$ transitions are included at up to 10% of the intensity of the $\Delta m_I = 0$ transitions.

IV. DISCUSSION

We observed structure due to ^{18}O, ^{37}Cl, and ^{2}H replacing ^{16}O, ^{35}Cl, and ^{1}H, respectively, in the ligand sites directly

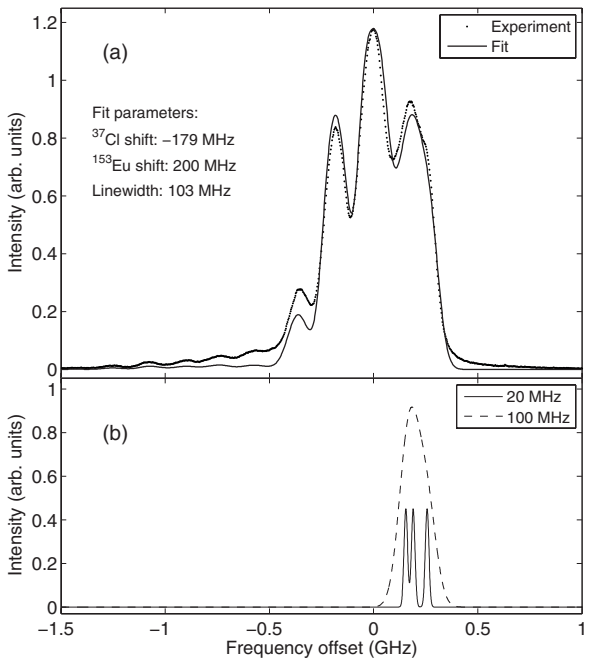

FIG. 4. (a) Least-squares fit to the excitation spectrum of the $^{7}F_0 \rightarrow {}^{5}D_0$ transition in natural abundance $EuCl_3 \cdot 6H_2O$. (b) Hyperfine structure of ^{153}Eu predicted from the fit in (a) with 20 and 100 MHz of inhomogeneous broadening.

surrounding the Eu ion. Features due to ^{17}O were not observed. It is likely that this was because of the low natural abundance of ^{17}O. We expect structure from ^{17}O with shifts smaller than those of ^{18}O, and intend to grow a ^{17}O-enriched crystal to confirm this. The ratio of the ^{17}O:^{18}O shifts could help study the mechanism producing the shifts.

Isotopes at sites outside of the immediate ligand environment will also contribute to the spectrum, causing inhomogeneous broadening. Given that an increase from 0.2% to 1.9% ^{18}O results in an additional 30 MHz of inhomogeneous broadening, we expect that the 24% ^{37}Cl in the crystal is the major source of broadening and no substantial reduction in the linewidth can be achieved without removing ^{37}Cl.

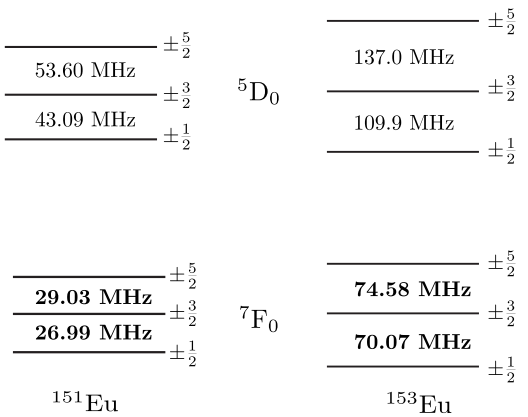

FIG. 5. Hyperfine structure of $^{7}F_0$ and $^{5}D_0$ for ^{151}Eu and ^{153}Eu. The values in bold were measured in this experiment and the remainder are those of Martin *et al.* (Ref. 13). The ordering of the ground state is opposite to Martin *et al.*

In order to fit the spectrum we required that the ordering of hyperfine levels be the same in the ground and excited states. This ordering is different to Martin *et al.*,[13] who proposed a reversed ordering, but is not contradicted by the data in their paper. A reversed ordering is possible in Eu because the zero-field spin Hamiltonian of the ground state has both quadrupole and pseudoquadrupole terms, which can have opposite signs, while the excited state is dominated by the quadrupole term. The ratio of excited-state splittings in ^{153}Eu and ^{151}Eu, therefore, gives the ratio of quadrupole moments for the two isotopes. In $EuCl_3 \cdot 6H_2O$ $^{153}Q/^{151}Q=2.55$, which is in good agreement with previous measurements (e.g., Ref. 14). The ratio of splittings in the ground state is 2.58 and the small deviation of this ratio from 2.55, the value expected for a pure quadrupole interaction, suggests that the pseudoquadrupole interaction is weak. This supports the assignment of same ordering in ground and excited states.

The fit in Fig. 4(a) showed that the $^7F_0 \rightarrow {}^5D_0$ transition is dominated by $\Delta m_I=0$ components with $\Delta m_I=1$ components contributing less than 10%. In an isotopically pure crystal of $^{153}Eu^{35}Cl_3 \cdot 6\,{}^1H_2{}^{16}O$, therefore, the spectrum of the $^7F_0 \rightarrow {}^5D_0$ transition would be made up of only three components of the hyperfine structure of ^{153}Eu and at inhomogeneous linewidths of less than 20 MHz these would be well resolved, as shown in Fig. 4(b).

As explained above, ^{37}Cl is a major source of broadening in $EuCl_3 \cdot 6H_2O$. It is possible, therefore, that an isotopically pure $EuCl_3 \cdot 6H_2O$ crystal will have an inhomogeneous linewidth less than 20 MHz and completely resolved hyperfine structure. Given this, we will briefly discuss the advantages of using a material with fully resolved hyperfine structure for a gradient echo quantum memory.[3,15]

In a gradient echo quantum memory, a spatial electric or magnetic-field gradient is applied to a crystal with a very narrow, optically thick absorption feature. This creates a spatial gradient in the frequency of the absorption feature, due to the Stark effect in the case of an electric field or the Zeeman effect for a magnetic field. When a pulse of light is sent into the material, different frequency components are absorbed at different spatial positions. To retrieve the stored pulse the direction of the electric or magnetic-field gradient is switched and the pulse is emitted in the forward direction.[15] Importantly, throughout this process the light interacts with only one edge of the absorption feature; for the operation of the memory an absorption feature with one sharp edge is sufficient. In a crystal with large inhomogeneous broadening, the narrow absorption feature is created by using optical pumping to burn a trench in the optical transition, and then to create a narrow feature in the middle of this trench. As the narrow feature cannot be frequency shifted by more than the width of the trench, the bandwidth of the quantum memory is limited by the trench width, which is limited by the hyperfine structure. This is not the case for a crystal with a narrow linewidth and completely resolved hyperfine structure. Either the highest or lowest frequency hyperfine component is used as the sharp edge of the absorption feature and the only limit on the bandwidth of the memory is the maximum field that can be applied to the material. The hyperfine structure is not a fundamental limit on the bandwidth of the memory, contrary to a conclusion of the original gradient echo quantum memory theory paper.[15]

In conclusion, we have observed partially resolved structure with 100 MHz of inhomogeneous broadening in the spectrum of the $^7F_0 \rightarrow {}^5D_0$ transition of $EuCl_3 \cdot 6H_2O$, and have shown that it is caused by isotopes of the ligands Cl, O, and H. We have measured the Eu isotope shift and isotope shifts caused by the ligands O and H using Raman-heterodyne-detected NMR. We have successfully modeled the structure as a combination hyperfine structure of the two Eu isotopes with shifts caused by Cl and O isotopes and with the ordering of hyperfine levels the same in ground and excited states. There is strong evidence that the inhomogeneous linewidth of the optical transition can be reduced to below the hyperfine splitting by using isotopically pure materials. If possible this would remove a significant constraint on the bandwidth of gradient echo memories.

ACKNOWLEDGMENTS

The authors acknowledge the support of the Australian Research Council.

[1] T. Bottger, C. W. Thiel, R. L. Cone, and Y. Sun, Phys. Rev. B **79**, 115104 (2009).
[2] E. Fraval, M. J. Sellars, and J. J. Longdell, Phys. Rev. Lett. **95**, 030506 (2005).
[3] A. L. Alexander, J. J. Longdell, M. J. Sellars, and N. B. Manson, Phys. Rev. Lett. **96**, 043602 (2006).
[4] J. J. Longdell, E. Fraval, M. J. Sellars, and N. B. Manson, Phys. Rev. Lett. **95**, 063601 (2005).
[5] H. de Riedmatten, M. Afzelius, M. U. Staudt, C. Simon, and N. Gisin, Nature (London) **456**, 773 (2008).
[6] T. Chanelire, J. Ruggiero, M. Bonarota, M. Afzelius, and J. L. L. Gout, arXiv:0902.2048 (unpublished).
[7] N. I. Agladze, M. N. Popova, G. N. Zhizhin, V. J. Egorov, and M. A. Petrova, Phys. Rev. Lett. **66**, 477 (1991).
[8] R. M. Macfarlane, R. S. Meltzer, and B. Z. Malkin, Phys. Rev. B **58**, 5692 (1998).
[9] R. M. Macfarlane, A. Cassanho, and R. S. Meltzer, Phys. Rev. Lett. **69**, 542 (1992).
[10] N. K. Bel'skii and Yu. T. Struchkov, Sov. Phys. Crystallogr. **10**, 15 (1965).
[11] N. C. Wong, E. S. Kintzer, J. Mlynek, R. G. DeVoe, and R. G. Brewer, Phys. Rev. B **28**, 4993 (1983).
[12] M. Yamaguchi and T. Suemoto, J. Phys. Soc. Jpn. **72**, 429 (2003).
[13] J. P. D. Martin, M. J. Sellars, P. Tuthill, N. B. Manson, G. Pryde, and T. Dyke, J. Lumin. **78**, 19 (1998).
[14] W. R. Babbitt, A. Lezama, and T. W. Mossberg, Phys. Rev. B **39**, 1987 (1989).
[15] B. Kraus, W. Tittel, N. Gisin, M. Nilsson, S. Kroll, and J. I. Cirac, Phys. Rev. A **73**, 020302(R) (2006).